1 10 Residual Contributors Included in Fit

1.1 What the fuck

This section presents fit results for which 10 residual contributors were assumed. These contributors include those shared by the three contributor case (App. **??**), (Σ^0K, Ξ^0K, Ξ^-K) $\rightarrow$ ΛK, and additionally the contributors ($\Sigma^{*(+,-,0)}$K^{*0}, ΛK^{*0}, Σ^0K^{*0}, Ξ^0K^{*0}, Ξ^-K^{*0}) $\rightarrow$ ΛK. As stated at the beginning of App. **??**, most of the Σ^* and K* resonances will have decayed before kinetic freeze-out, and therefore it is best to treat Λ and K particles originating from these resonances as primary, i.e. only using three residual contributors. However, it is still interesting to examine how these additional shorter lived sources affect our fit result, as presented below. For a comparison of these results to the case of three residual contributors, see Fig. **??** in App. **??**

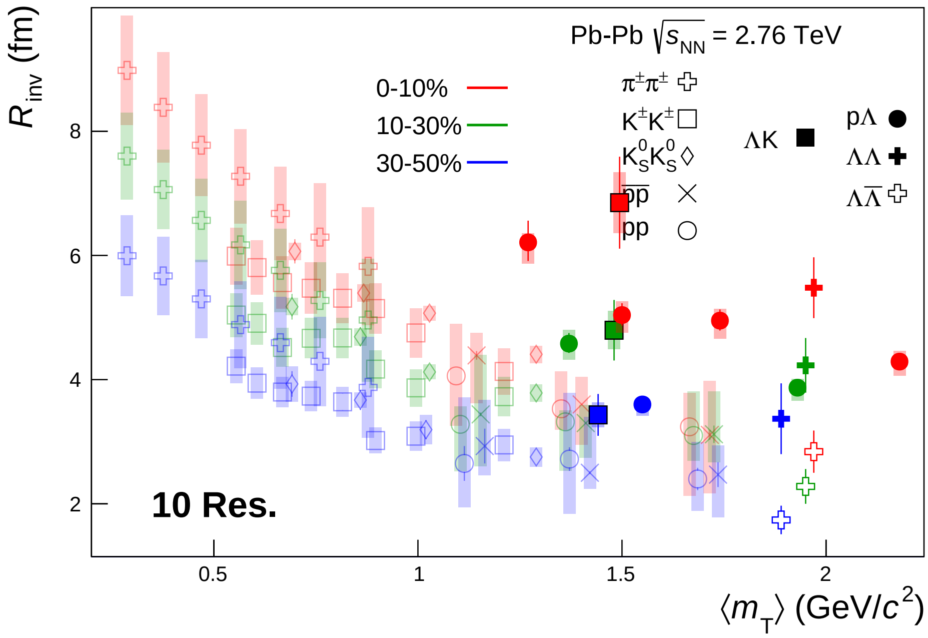

Fig. 1: 10 residual correlations in ΛK fits. Extracted fit R_{inv} parameters as a function of pair transverse mass (m_T) for various pair systems over several centralities. The ALICE published data [**?**] are shown with transparent, open symbols. The new ΛK results are shown with opaque, filled symbols. The m_T value for the ΛK system is an average of those for the ΛK$^+$, $\bar{\Lambda}$K$^-$, and ΛK^0_S systems.

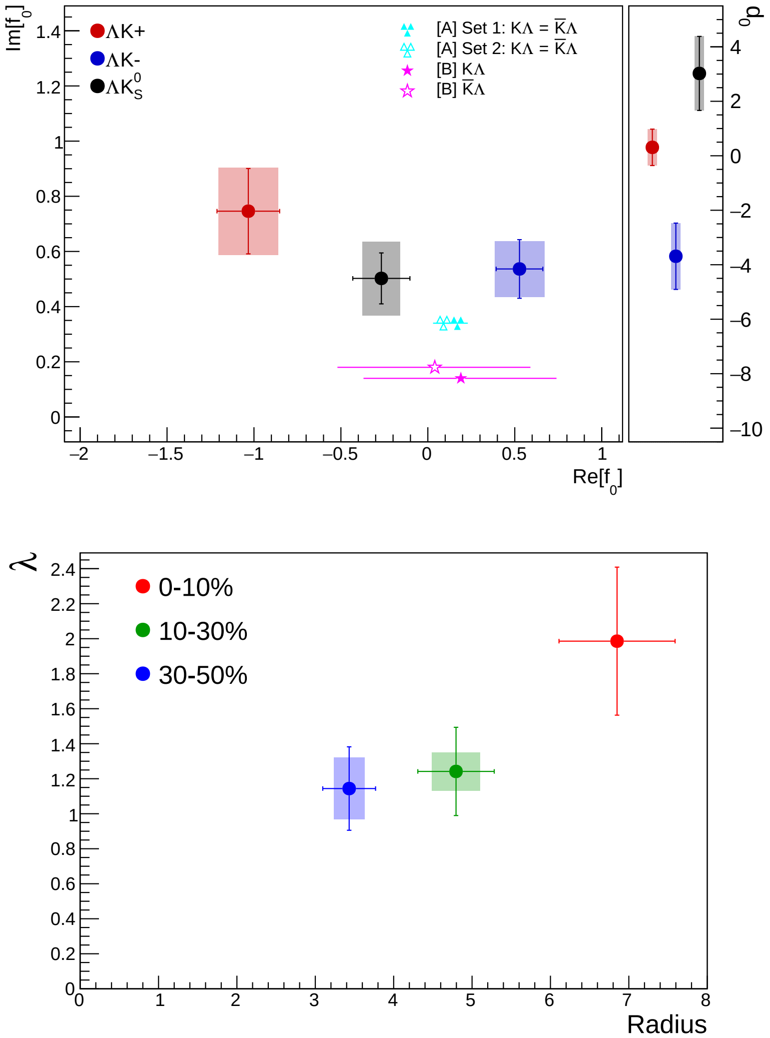

Fig. 2: Extracted fit parameters for the case of 10 residual contributors for all of our ΛK systems. [Top]: $\Im f_0$ vs. $\Re f_0$, together with d_0 to the right. [Bottom]: λ vs. Radius for the 0-10% (blue), 10-30% (green), and 30-50% (red) centrality bins. In the fit, all ΛK systems share common radii. The color scheme used in the panel are to be consistent with those in Fig. 1. The cyan ([A] = Ref. [**?**]) and magenta ([B] = Ref. [**?**]) points show theoretical predictions made using chiral perturbation theory.

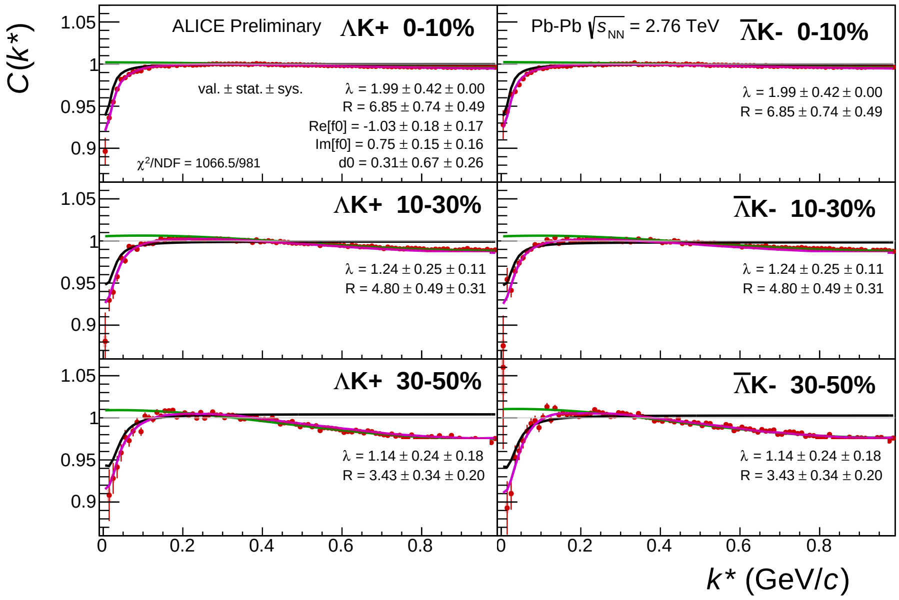

Fig. 3: Fit results, with 10 residual correlations included, for the ΛK^+ and $\bar{\Lambda}K^-$ data. The ΛK^+ data is shown in the left column, the $\bar{\Lambda}K^-$ in the right, and the rows differentiate the different centrality bins (0-10% in the top, 10-30% in the middle, and 30-50% in the bottom).

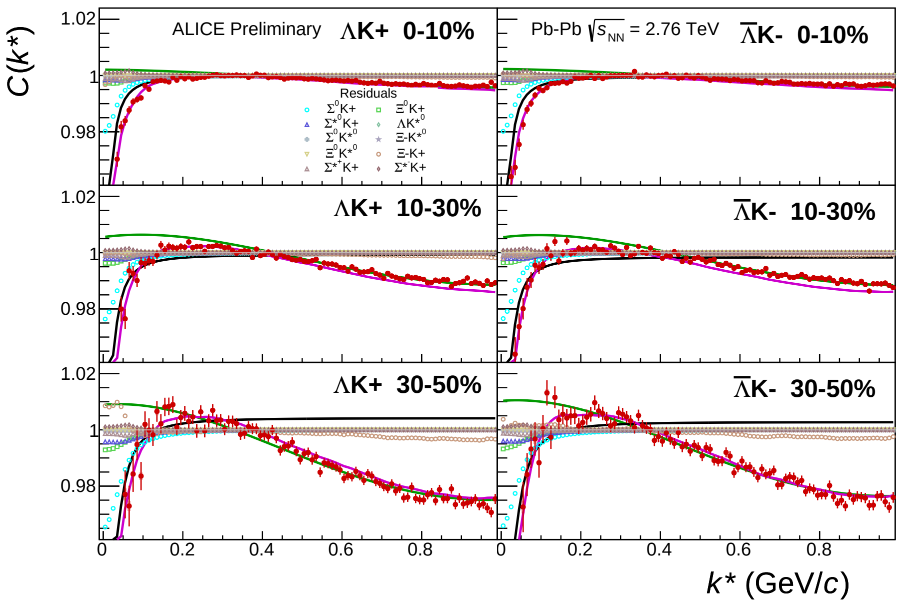

Fig. 4: Fit results with the 10 residual contributions shown, for the ΛK^+ and $\bar{\Lambda}K^-$ data. The ΛK^+ data is shown in the left column, the $\bar{\Lambda}K^-$ in the right, and the rows differentiate the different centrality bins (0-10% in the top, 10-30% in the middle, and 30-50% in the bottom).

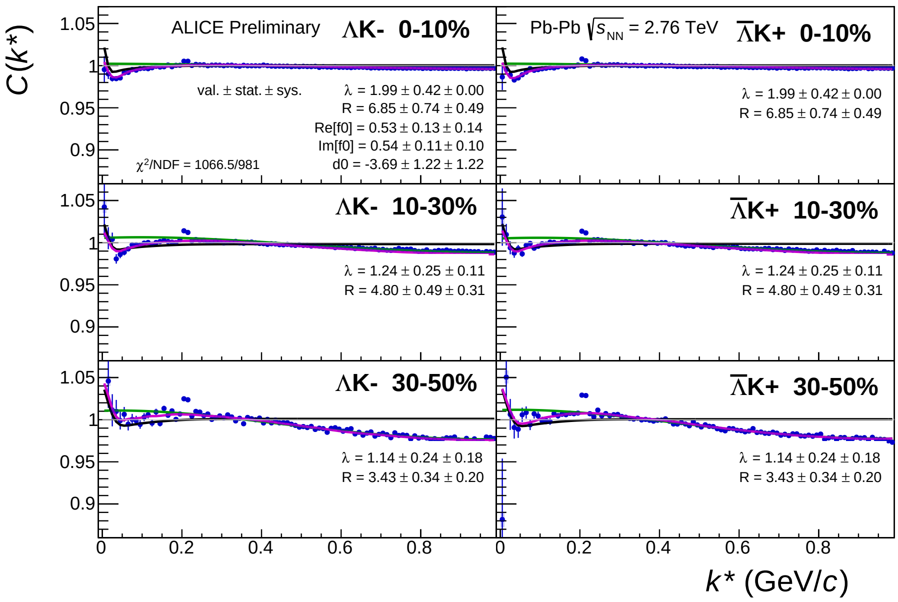

Fig. 5: Fit results, with 10 residual correlations included, for the ΛK^- and $\bar{\Lambda}K^+$ data. The ΛK^- data is shown in the left column, the $\bar{\Lambda}K^+$ in the right, and the rows differentiate the different centrality bins (0-10% in the top, 10-30% in the middle, and 30-50% in the bottom).

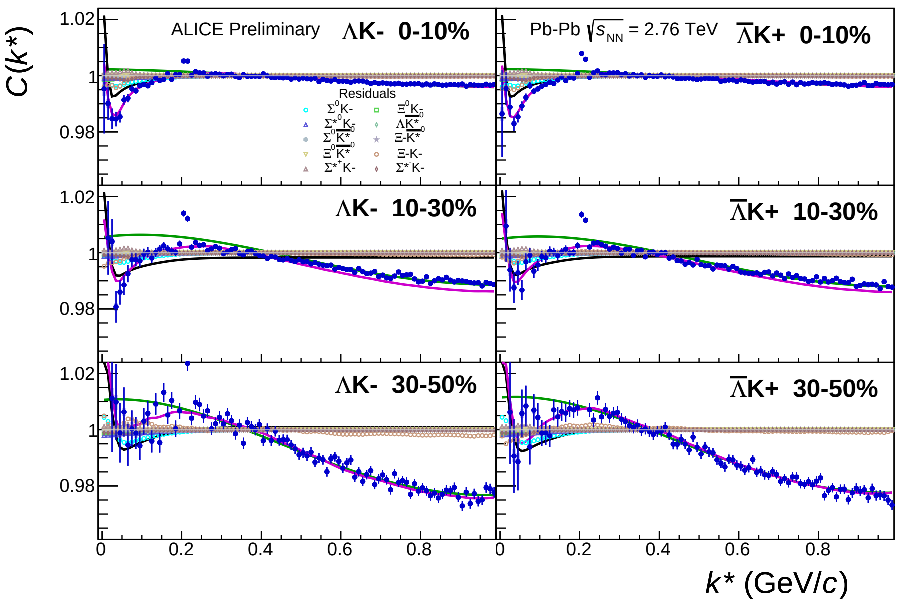

Fig. 6: Fit results with the 10 residual contributions shown, for the ΛK^- and $\bar{\Lambda}K^+$ data. The ΛK^- data is shown in the left column, the $\bar{\Lambda}K^+$ in the right, and the rows differentiate the different centrality bins (0-10% in the top, 10-30% in the middle, and 30-50% in the bottom).

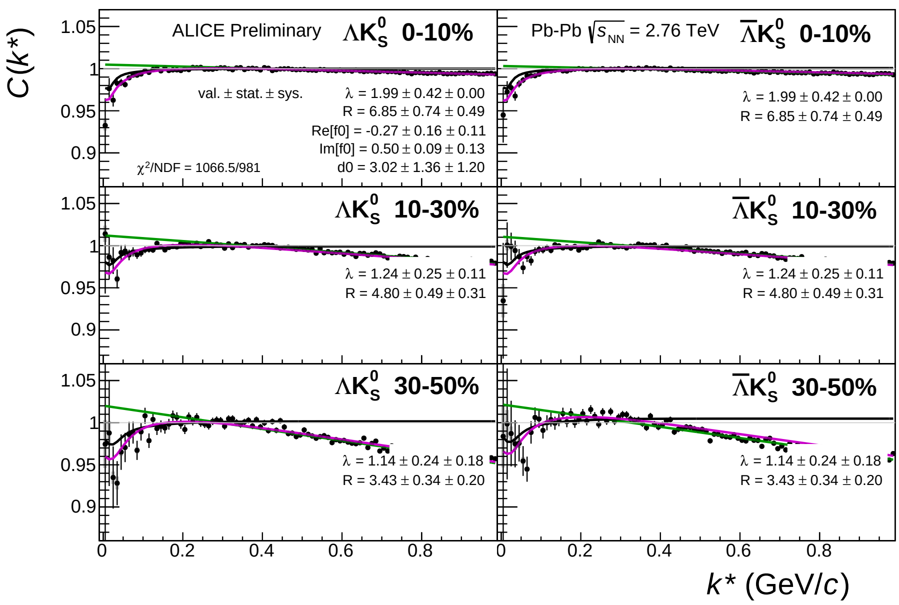

Fig. 7: Fit results, with 10 residual correlations included, for the ΛK^0_S and $\bar{\Lambda}K^0_S$ data. The ΛK^0_S data is shown in the left column, the $\bar{\Lambda}K^0_S$ in the right, and the rows differentiate the different centrality bins (0-10% in the top, 10-30% in the middle, and 30-50% in the bottom).

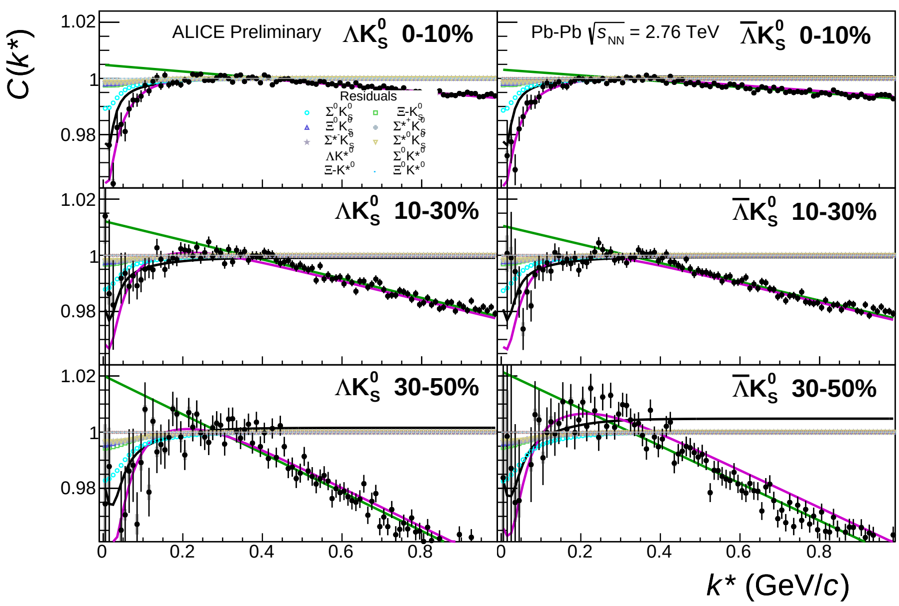

Fig. 8: Fit results with the 10 residual contributions shown, for the ΛK^0_S and $\bar{\Lambda}K^0_S$ data. The ΛK^0_S data is shown in the left column, the $\bar{\Lambda}K^0_S$ in the right, and the rows differentiate the different centrality bins (0-10% in the top, 10-30% in the middle, and 30-50% in the bottom).